Journal of Molecular Liquids 346 (2022) 117157

Contents lists available at ScienceDirect

Journal of Molecular Liquids

journal homepage: www.elsevier.com/locate/molliq

Remdesivir interactions with sulphobutylether-β-cyclodextrins: A case study using selected substitution patterns

Ángel Piñeiro [a], James Pipkin [b], Vince Antle [b], Rebeca Garcia-Fandino [c,*]

[a] Departamento de Física de Aplicada, Facultade de Física, Universidade de Santiago de Compostela, E-15782 Santiago de Compostela, Spain
[b] Ligand Pharmaceuticals Incorporated, 3911 Sorrento Valley Boulevard, San Diego, CA, USA
[c] Departamento de Química Orgánica, Center for Research in Biological Chemistry and Molecular Materials, Universidade de Santiago de Compostela, Campus Vida s/n, E-15782 Santiago de Compostela, Spain

ARTICLE INFO

Article history:
Received 7 April 2021
Revised 26 July 2021
Accepted 29 July 2021
Available online 12 August 2021

Keywords:
Cyclodextrins
Remdesivir
ITC
PMF
Molecular dynamics
Association constant

ABSTRACT

Modified cyclodextrins (CDs) consist of a distribution of different structures with different number and location of the substituted groups. Among the most important applications of these molecules is their use as an enabling excipient in pharmaceutical formulations to provide the necessary solubility, stability and bioavailability for a drug to be effectively used. The most typical interaction mechanism of small molecular groups with CDs is the formation of host–guest inclusion complexes. The thermodynamic affinity constant between CDs and drugs should not be too strong, since then the biological activity could be negated by the formation of the complex. In the opposite scenario, if the affinity constant is too weak, the complex is barely formed and the amount of CD required in the formulation may become too great. Thus, a balance between the affinity of the CD and the drug is necessary for an optimal formulation. Additionally in the case of modified CDs and specific drug complexes there are further questions concerning the effect that the locations and number of substitutions plays in complexation. In the present work, this question is explored by using sulphobutylether-β-cyclodextrin and remdesivir, the only antiviral medication currently approved by the United States Food and Drug Administration for treating COVID-19, as a case study. This paper presents results from an orthogonal study using isothermal titration calorimetry measurements and biased molecular dynamics simulations that provide complementary information. Isothermal titration calorimetry delves into the global impact of the species distribution while molecular dynamics simulations deals with specific chemical structures. The goal is to provide useful information to optimize pharmaceutical formulations based on modified CDs, specifically in the case of remdesivir, used to treat SARS-CoV-2 infection, although the main conclusions could be extended to the interaction of other drugs with modified cyclodextrins.

1. Introduction

Remdesivir (Fig. 1) is the active principle of VEKLURY®, the only antiviral medication currently approved by the United States Food and Drug Administration (FDA) for treating COVID-19 (https://www.fda.gov/newsevents/press-announcements/fda-approves-first-treatment-covid-19). Other countries including Japan, United Kingdom, South Korea, Taiwan, India, Singapore, Israel, the European Union and Australia have also regulated the use of this drug with different restriction levels (https://www.reuters.com/article/healthcoronavirus-gilead-remdesivir-idUSL4N2EA2LZ). Remdesivir was developed by Gilead Sciences over a decade ago to treat Hepatitis C and respiratory syncytial virus (https://www.gilead.com/-/media/gileadcorporate/files/pdfs/covid-19/gilead_rdv-development-fact-sheet-2020.pdf). Although it proved to be ineffective for these diseases, it was repurposed as a potential treatment for Ebola [1] and other infections including those caused by several coronaviruses: Middle East Respiratory Syndrome (MERS) and Severe Acute Respiratory Syndrome (SARS) [2,3]. Remdesivir prevents the replication of the virus by inhibiting the RNA-dependent RNA polymerase (RdRp) [4,5], which is a key enzyme for that mechanism [6]. Thus, at the outset of the appearance of the SARS-CoV-2 pandemic, remdesivir was immediately considered a potential treatment against COVID-19. Some debate exists about the efficacy of this drug [7] although it has been clinically proved that the recovery time of the patients affected by this disease is significantly reduced after a 5 days treatment [8]. Longer duration of use are not recommended since the potential benefit

* Corresponding author.
E-mail address: rebeca.garcia.fandino@usc.es (R. Garcia-Fandino).

https://doi.org/10.1016/j.molliq.2021.117157
0167-7322/

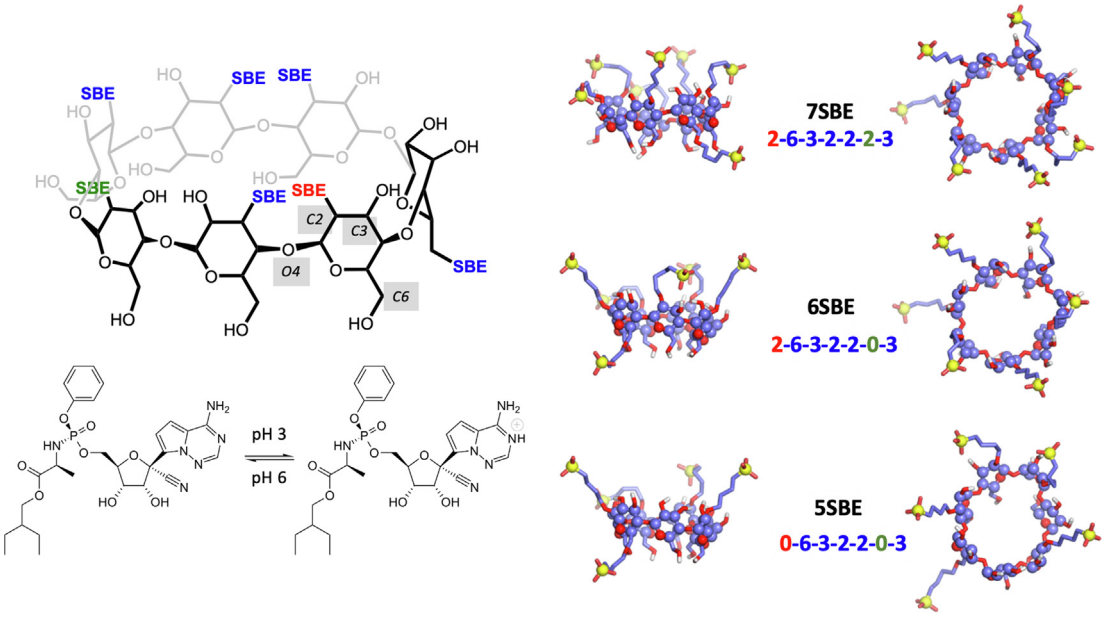

Fig. 1. Left: 2-dimensional representation of SBE-β-CD and the equilibrium between neutral and protonated remdesivir. In the CD structure the blue labels represent the groups that are substituted in all the structures studied by MD simulations, the red label represents the group that is substituted in **6SBE** and in **7SBE** and the green label represent the group that is substituted also in **7SBE**. The labels with grey background represent the position of the carbon atoms *C2*, *C3* and *C6* and that of the oxygen *O4*. Right: Three dimensional representations of the β -CD structures with 7, 6 and 5 SBE substitutions employed for the MD simulations. Carbon atoms are represented in violet, oxygens in red, hydrogens in white, and sulphur atoms in yellow. Atoms of the glucopyranoside rings and sulphurs are in spheres while other oxygen and carbon atoms are in stick representation. Two different views of each structure are shown. The label indicates the counter-clockwise sequence of substitutions, when the CD structure is oriented as in the second column of the figure, with the secondary hydroxyl groups pointing out of the plane. The numbers 2, 3 or 6 represent the position of the substitution group in each glucopyranoside ring and 0 indicates that no substitution is present in the corresponding ring. The color code is the same as that used in the left upper figure. (For interpretation of the references to color in this figure legend, the reader is referred to the web version of this article.)

does not compensate for the observed hepatocellular injury in healthy volunteers and COVID-19 patients treated with this antiviral drug [9].

The pharmaceutical formulation of remdesivir includes sulphobutylether β-cyclodextrins (SBE-β-CD) as an excipient to address the limited solubility and stability of this drug. In general, modified cyclodextrins are highly versatile molecules where the primary or/and secondary hydroxyl groups of native cyclodextrins are substituted by other functional groups to improve their utility and safety. All these molecules share a common scaffold formed by 6–8 glucopyranoside groups covalently bound leading to a supraring with an internal hydrophobic cavity. They have been used in a large range of applications, many of them involved in coronavirus treatments [10]. The most typical application is the solubility increase of poorly soluble molecules when both solutes are jointly dissolved in water [11–15]. The encapsulation of hydrophobic groups in the cavity of the cyclodextrin forming inclusion complexes is typically assumed to be the interaction mechanism for this application [16,17]. In some cases, the encapsulated molecule is protected from chemical degradation. When using a CD for these purposes (solubilize and stabilize a given molecule) it is key to quantify the affinity between both compounds and also to know the structure of the resulting supramolecular complex. A very large affinity constant is not convenient because in that case the active molecule may not be released as desired, so it could not carry out its function. In contrast, if the encapsulation is negligible, the solubility increase and protection against degradation would be inefficient.

The structural and thermodynamic characterization of inclusion complexes between native CDs and different molecules can be done by different experimental and computational methods and, in general, it is relatively easy to perform and interpret when the materials are single chemical species. In the case of modified CDs the presence of multiple and different substitution patterns that make up the modified CD material introduces an additional and non-trivial-to-solve complexity. In particular, it is known that the derivatization of cyclodextrins with sulfoalkyl groups occurs in a controlled although not exact manner. For this reason, SBE-β-CD is a mixture of both positional and regioisomers, the degree of substitution (DS) representing the average number of functional groups per CD. Moreover, substitution of the different hydroxyl groups occurs during manufacture of the derivatized CD, so the average molecular weight of the final composition may vary from batch to batch. Such a distribution represents a galaxy of molecular structures with a common scaffold but with different number and location of substitutions, different molecular weight, different diffusion properties and solvation energy, and potentially have different ability to encapsulate a given ligand [18,19]. Explicitly considering the distribution of species in a structural and thermodynamics analysis of inclusion complexes is not trivial, so classical experiments provide representative parameters for the whole material. Having a better understanding on how the encapsulation depends on the substitution pattern could boost the development of new manufacturing processes able to optimize the formulation of these excipients for specific drugs. This is important to learn how to minimize exposure and risk to the kidney hypothetically attributed to the accumulation of SBE-β-CD in really compromised COVID-19 patients treated with remdesivir [20,21].

To our knowledge, the thermodynamic characterization for the formation of supramolecular complexes between remdesivir and SBE-β-CD has not been performed and the resulting structures have not been described in detail. Different molar concentration ratios of both solutes (CD:drug) were tested to design the pharmaceutical formulations of remdesivir but typical mass ratio values range from 10:1 to 30:1 [22] and the VEKLURY Injection ready-made solution presentation has a mole ratio of 16.7:1 and a mass

ratio of 60:1 (VEKLURY PI 2020). Based on the linear dependence of the drug solubility as a function of the CD concentration, the formation of 1:1 complexes between these two compounds has been proposed [22]. Thus, the need for such a large proportion of CD in the formulation suggests that the binding is not very strong. The mixture between both molecules is preferentially performed at low pH since the solubility of remdesivir, pKa 3.3 (https://www.ema.europa.eu/en/documents/assessment-report/veklury-epar-public-assessment-report_en.pdf) significantly increases under this condition [22]. It was observed that the drug remains encapsulated upon the addition of NaOH at the proposed concentrations, although a weakness of the complex was expected when increasing the pH [22].

The present work is intended to shed some light on this issue by combining the analysis of multiple isothermal titration calorimetry (ITC) experiments at two different pH values with biased molecular dynamics (MD) simulations using neutral and protonated remdesivir, as well as three different structures for SBE-β-CD with 5, 6 and 7 substituted groups.

2. Materials and methods

2.1. Materials

SBE-β-CD and remdesivir were provided by the CyDex subsidiary of Ligand Pharmaceuticals and employed without further purification. The commercial name of this cyclodextrin is CAPTISOL®. All the solutions were prepared by weight, using citrate buffer previously adjusted at the desired pH using NaOH/HCl. Millipore water was employed to prepare the buffer.

2.2. Isothermal titration calorimetry (ITC) experiments

In order to get a thermodynamic characterization for the interaction between SBE-β-CD and remdesivir, ITC experiments were performed using a VP-ITC instrument from Microcal with a sample cell of 1.4323 mL. Since the solubility of remdesivir is low and significantly dependent on the pH experiments at pH 6 and at pH 3 were carried out, where the drug is expected to be neutral and positively charged, respectively. At pH 3 all the experiments were performed using a 0.1 mM solution of the drug and different concentrations of the modified cyclodextrin: 1, 1.5, 2.5 and 5 mM. The concentration of remdesivir at pH 6 was reduced to 0.03 mM and the employed solutions of SBE-β-CD were 0.3, 1.0 and 2.5 mM. Considering the limited solubility of remdesivir, even at low pH, it was placed in the sample cell of the instrument in all the experiments since the compound in the syringe typically requires ~ 10 times higher concentration. One small injection of 1 μL followed by 28 × 10 μL aliquots of each cyclodextrin solution were then injected in the remdesivir solution. Dilution experiments of the CD in buffer were performed for all the concentrations. The measurements were analyzed using the AFFINImeter software (www.affinimeter.com; Piñeiro, et al. 2019).

2.3. Molecular dynamics (MD) simulations

The SBE-β-CD provided by Ligand Pharmaceuticals (CAPTISOL) is a distribution of modifiedβ-CDs with different number and location of SBE substitutions with an average substitution number of 6.5. For the MD simulations, 3 different representative component structures of SBE-β-CD with a single substitution on the primary side and 4, 5 or 6 substitutions in the secondary side of the CD (see Fig. 1) were selected: **5SBE**, **6SBE** and **7SBE**, respectively. These structures were considered to be suitable to examine the role of Degree of Substitution (DS), considering these are three of the larger DS fractions of CAPTISOL, NMR studies on file at CyDex showed ~ 85% of the substitution is on the secondary side with slightly greater than 3 to 2 ratio of substitutions at the -2 versus -3 positions, and using a rule for this comparison that no more than one substitution can take place in a single glucose unit. Note that for low substitution numbers the secondary hydroxyls are more prone to be substituted [23,24]. For remdesivir the neutral structure and the protonated structure as shown in Fig. 1 were used.

Using these structures, potential of mean force (PMF) profiles for the formation of inclusion complexes with neutral and protonated remdesivir were determined. These simulations are computationally expensive compared with standard non-biased MD simulations starting from specific conformations of the complexes but, in return, they allow to effectively sampling the accessible degrees of freedom as a function of a given reaction coordinate. The aim of these calculations is to get the energy barriers and wells as a function of the reaction coordinate, an estimation of the binding constant and the most likely structures for each complex.

2.3.1. General simulation methods

The simulation parameters are similar to those employed in previous works for similar systems [25,26]. All the simulations were performed using the GROMOS 54a7 force field [27] (Schmid, et al. 2011) with SPC water molecules [28] and the GROMACS 2020 engine [29,30]. The initial coordinates for the independent molecules and the topologies were built using our own tools. All the simulations were performed using the NPT ensemble at 298 K and 1 bar. The temperature and pressure were controlled using the v-rescale thermostat [31] and the Parrinello-Rahman barostat [32] with coupling constants of 0.1 and 0.5 ps, respectively. The long range interactions were determined using the Particle Mesh Ewald algorithm [33,34] with a grid spacing of 0.15 nm and a direct-space cutoff of 1.2 nm. The same cutoff was employed for the short-range interactions. A timestep of 2 fs was employed in all cases using the leap-frog integrator algorithm [35]. All bonds were constrained using the SETTLE algorithm [36] for water and the LINCS algorithm [37] for the CDs and the remdesivir molecules.

2.3.2. Umbrella Sampling simulations

The PMF profile for the interaction between each pair of molecules was independently obtained with the remdesivir structure initially oriented in opposite directions (“up” and “down”) within the CD cavity (Fig. 2). The reaction coordinate (ξ) is the distance between the center of mass (COM) of the *O4* atoms of the CD and the COM of the whole remdesivir molecule. In order to build the initial structures for the PMF calculations, the drug was initially placed just in the middle of the CD cavity and then it was sequentially displaced in small 0.02 nm steps towards both the primary and the secondary sides of the CD up to 2.5 nm in each direction (Fig. 2). Thus, a total of 500 different frames with different relative orientations and ξ values were obtained for each pair of structures: neutral or protonated remdesivir and the three CDs: **7SBE**, **6SBE** and **5SBE**. These structures were inserted in dodecahedron boxes with 7-nm-long side axis, large enough to prevent interactions with periodic images even at the largest distances between solute molecules. The simulations boxes corresponding to the same structures were solvated with exactly the same number of SPC water molecules (approximately 7800 for all systems after removing those overlapping the solute atoms). Then, a steepest descent minimization was performed for all boxes with a force constant of 10^4 $kJ{\cdot}mol^{-1}{\cdot}nm^{-2}$ to constrain the initial value of the reaction coordinate in each case. The structure resulting from this minimization was employed to obtain 15-ns-long umbrella sampling simulations with a force constant of 3000 $kJ{\cdot}mol^{-1}{\cdot}nm^{-2}$. This value was selected after several tests and it was considered to be large enough to keep the constrained reaction coordinate value at rea-

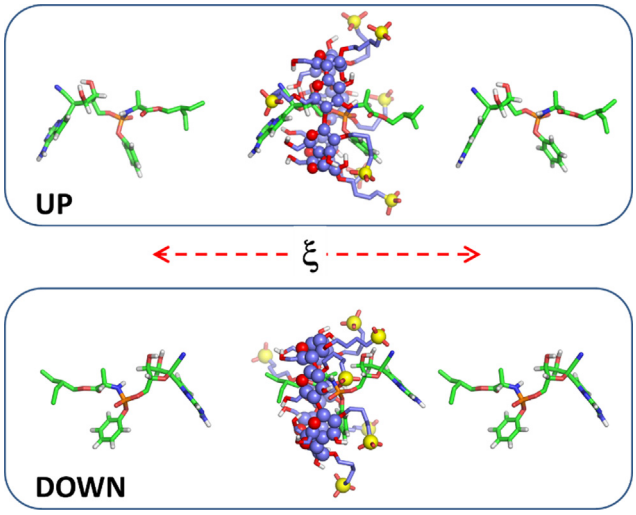

Fig. 2. Representations of the reaction coordinate (ξ) used for the umbrella sampling calculations, for the "up" and "down" relative orientations between the cyclodextrin and the remdesivir molecules. The colors, as well as the sphere and stick representations for the cyclodextrin are as in Fig. 1. For remdesivir the carbon, oxygen, hydrogen and nitrogen atoms are in green, red, white and blue, respectively. (For interpretation of the references to color in this figure legend, the reader is referred to the web version of this article.)

sonably unfavourable conformations and short enough to produce reasonably wide distance and force distributions so that a reasonable overlapping can be obtained. The distance between the COM of the ligand and that of the *O4* atoms of the CD, as well as the force required to constrain the selected distance between both structures were stored every 0.1 ps for further analysis. A total of 3000 × 15-ns-long trajectories (45 μs in total) were performed.

2.3.3. Analysis of the trajectories

The PMF profiles were independently obtained by two different methods: (*i*) first we used the Weighted Histogram Analysis Method (WHAM), as implemented in the GROMACS package; (*ii*) as an alternative, the direct integration of the average force for each restrained simulation as a function of the reaction coordinate was also used. The second method is equivalent to the analysis typically performed in the Adaptive Biasing Force (ABF) method [38], although the sampling is performed in a different way, by constraining the reaction coordinate at specific values by a harmonic potential. These calculations were applied to each set of 250 trajectories corresponding to one CD and one remdesivir molecule with a predefined relative orientation. Although the PMF profiles obtained from both methods were similar, those obtained from the direct integration of the forces exhibited significantly less noise when calculated over different time periods than those using WHAM, so only the results coming from the second method are shown in this work. The resulting profiles were post-processed to determine the standard equilibrium binding constant (1 M reference state) for the formation of inclusion complexes (K_A) using the following equations [39,40]:

$$K_A = \int e^{-E(\mathbf{r})/RT} d\boldsymbol{r} \quad (1)$$

where $E(\mathbf{r})$ is the PMF as a function of the relative coordinates between both molecules ($\mathbf{r}$), R is the gas constant and T is the temperature. By using cylindrical coordinates (ϕ, ρ, z), integrating the volume element over ϕ (from 0 to 2π) and ρ (from 0 to ρ_{av}), and taking z as the reaction coordinate (ξ), the following equation is obtained:

$$K_A = \pi N_A \int \rho_{av}^2(\xi) e^{-E(\xi)/RT} d\xi \quad (2)$$

In this equation $\rho_{av}(\xi)$ is the maximum distance between the COM of the remdesivir molecule and the axis defined by the reaction coordinate (see Fig. 2) for each simulation. This defines the radius of the accessible circle for each value of ξ. N_A is the Avogadro's number.

The uncertainties of the K_A values were estimated by using a bootstrapping method. Each 15-ns-long trajectory was distributed in 15 × 1-ns-long segments, then the PMF profile was obtained from all the trajectories corresponding to the same segment. The standard deviation of the resulting distributions was used to estimate the uncertainties. The values that differ from the mean by more than 1 standard deviation were removed in a single step before obtaining the final values. The typical number of outliers for each system was 2–3. Thus, the final association constants were determined using more than 10 × 1-ns-long trajectories in all cases.

3. Results & discussion

ITC measurements and MD simulations were used to characterize the interaction between remdesivir and SBE substituted β-CD. The commercial SBE-β-CD used in the ITC experiments (CAPTISOL®) is a heterogeneous mixture of many different chemical species with an average degree of substitution of 6.5. The number and location of the SBE groups are expected to affect the affinity of a specific CD structure for a given ligand. In a typical ITC experiment, the concentration of the CD gradually increases in the sample cell while the concentration of remdesivir is approximately constant [41]. Thus, the global impact of the species distribution should be reflected in a change in the value of the equilibrium constant during the titration experiment and, for the same reason, in different equilibrium constant values for experiments with different concentration of CD in the syringe. Whereas in ITC experiments it is not possible to distinguish the influence of each single CD unless they are isolated as reagents, MD simulations allow for carrying out specific studies with each particular substitution patterns. In this work, the calculations were performed using the structures shown in Fig. 1. Below, the results for the ITC and MD experiments will be presented and discussed.

3.1. ITC experiments

The experiments at pH 3 produced very clean power signals with a quick recovery of the perturbations due to the injections. The dilution titrations were very important in all cases and they should be explicitly considered in the model or directly subtracted from the raw measurements (Fig. 3).

The power raw data were integrated to determine the enthalpies and the dilution signals were subtracted to get the binding isotherms, which were then analyzed using different approaches:

- First, each isotherm was individually fitted to a simple 1:1 model. These fittings became overparameterized, supplying inconsistent values for the equilibrium association constants (K_A) and enthalpies (ΔH) as well as very large uncertainties. This is partially due to the low curvature of the isotherms which, when they are individually analyzed, do not seem to contain much information.
- Next, the number of degrees of freedom was drastically reduced by a global fitting of all the experimental data (with different concentrations of the cyclodextrin) together using a single set of K_A and ΔH. Using this approach, the experimental data considering was not able to be properly described using just 1:1

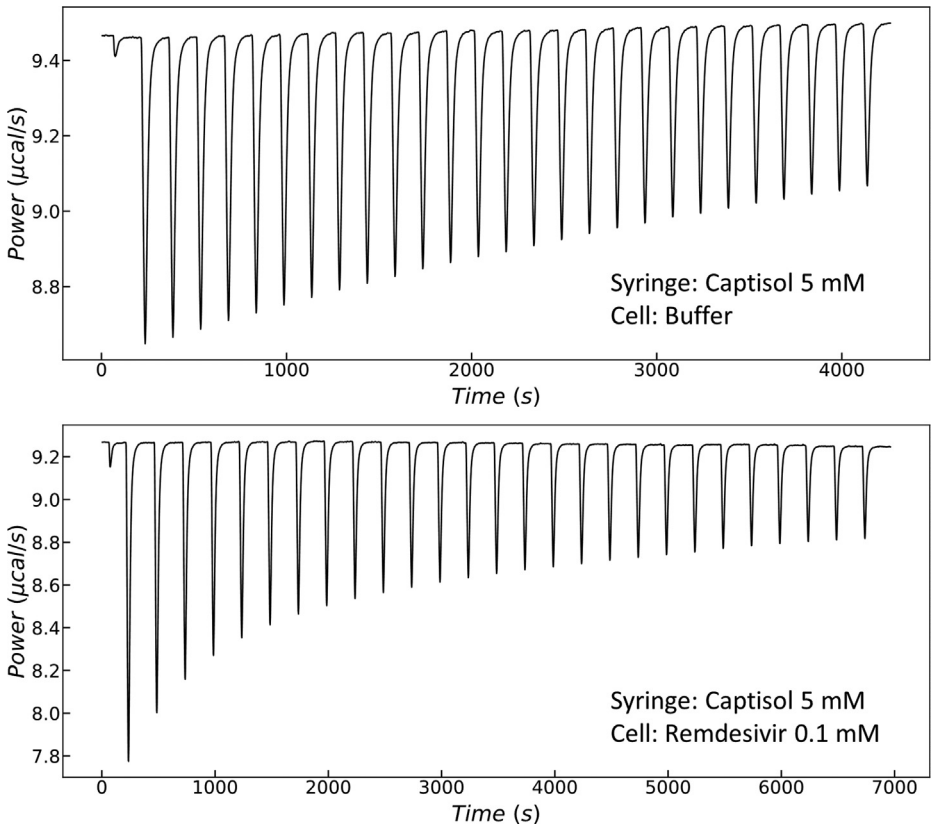

Fig. 3. ITC raw data corresponding to the titration of CAPTISOL (5 mM) in citrate buffer at pH 3 and in a 0.1 mM remdesivir solution.

complexes. So, it was concluded that this approach is also incorrect since the thermodynamic parameters describing a given interaction mechanism should not depend on the absolute/relative concentration of the involved chemical species. Since the signal to noise ratio of all the experiments is very low and the baseline after each injection is perfectly recovered, it is reasonable to assume that the equilibrium conditions are fulfilled and that a better model is needed to describe the experimental data. In this case, the most likely sources of discrepancy are the presence of a species distribution with different affinities in the SBE-β-CD compound or the interaction mechanism, that could include more complex stoichiometries or even some kind of aggregation.

- Later, it was decided to maintain the global fitting to a 1:1 model but introduce a correction factor for the concentration of CAPTISOL (r_C) as an approach to assess for the species distribution in this compound. Using this approach, a good description of the experimental data was obtained with r_C close to 2 and an apparent association constant of $6.56 \cdot 10^3$ M^{-1} (see Fig. 4 and Table 1). This r_C value could be interpreted as if half of the CAPTISOL distribution was inefficient to encapsulate the drug while the rest of the molecules exhibit the average affinity constant supplied by the fitting.
- An alternative explanation for the high r_C value obtained from the previous fitting could be the formation of 2:1 complexes (two CDs encapsulating each remdesivir molecule). In order to test this possibility, a global fitting was performed considering the presence of complexes with 2:1 stoichiometry and with $r_C = 1$. The resulting goodness of fit was 14% worse than that for the fitting shown in Fig. 3 and Table 1, even when the model including 2:1 species has one additional fitting parameter. Interestingly, the quality of the fitting considering 2:1 complexes was worse for the highest concentrations of CAPTISOL (2.5 and 5 mM), which are expected to be more sensitive to the eventual presence of higher order stoichiometries, than for the experiments using a CAPTISOL concentration of 1 or 1.5 mM. The parameters obtained for this second fitting are in Table 2. Even though the fitting to this second model is not as satisfactory as the fitting to the model shown in Fig. 3 and in Table 1, the association constants are of the order of 10^4 M^{-1} in both cases.

One hypothesis is that the high r_C value required to fit the 1:1 model arises from the variation of binding affinity along the species distribution of CAPTISOL. It is not trivial to model the variation of thermodynamic parameters along the distribution since they are expected to depend not only on the number of substituted groups but also on their location. This will be discussed later based on our MD calculations.

The signal to noise ratio of the experiments at pH 6 was significantly higher than for the experiments at pH 3. This is in part because the solubility of remdesivir is lower at higher pH [22] and so the experiments were performed at lower concentrations. As in the case of pH 3, the signal coming from the dilution of CAPTISOL is significant. In addition to the presence of noise, the binding isotherms at pH 6 do not exhibit a clear curvature and so, they are not very useful to discard different approaches, as was done with the experiments at pH 3. These results could be due to weak binding but they are not conclusive.

3.2. MD simulations

In contrast to ITC measurements, which provide a global apparent association constant for the whole distribution of CDs binding to remdesivir, MD simulations consider specific structures. Following the protocol described in the methodology section, the average

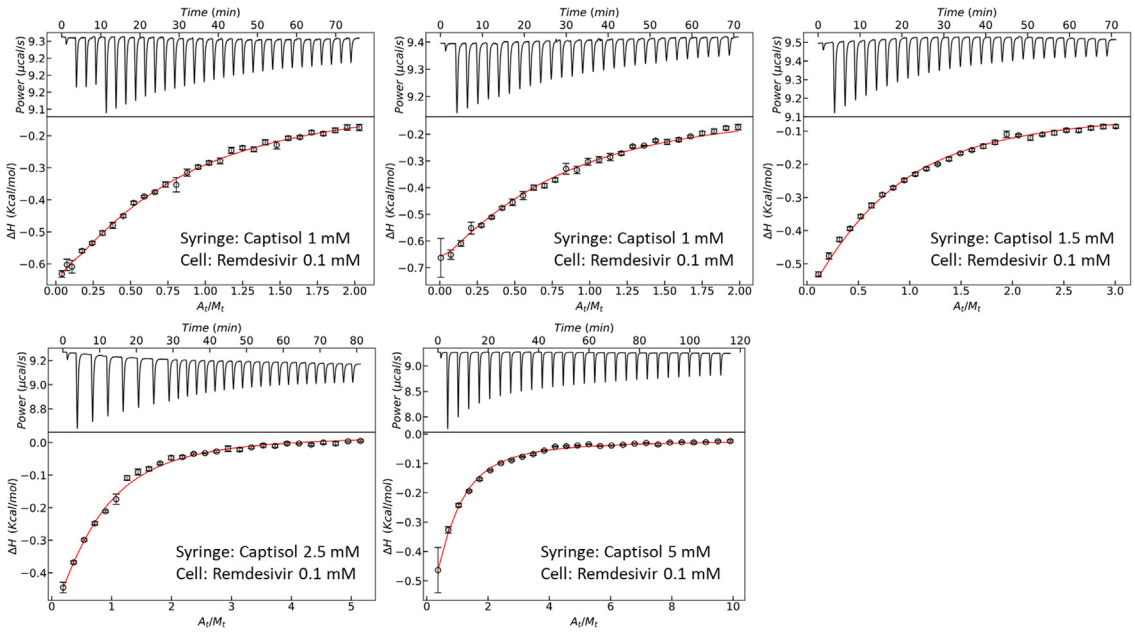

Fig. 4. Row data together with the binding isotherms and the curves resulting from a global fitting of the ITC experiments at pH 3. The employed concentrations of CAPTISOL and remdesivir are indicated in each plot. The signal corresponding to the dilution of CAPTISOL has been subtracted from all the binding isotherms in order to perform the fitting.

Table 1
Parameters resulting from a global fitting of a 1:1 model with a correction factor for the concentration of CAPTISOL (r_C) to the experimental ITC data at pH 3.

Parameter	Value	std dev
K_A (M^{-1})	6562	72
ΔH (cal/mol)	−678	2
r_C	1.905	0.009

Table 2
Parameters resulting from a global fitting of a 2:1 model to the ITC experimental data at pH 3. The corresponding chemical reactions are indicated in the first column. FS is the acronym for "Free Species", i.e. unbound CAPTISOL or remdesivir, C and R are used to represent the CAPTISOL and remdesivir molecules, respectively.

Reaction	Parameter	Value	std dev
FS ↔ C_1R_1	K_A (M^{-1})	9750	138
	ΔH (cal/mol)	−975	7
C_1R_1 + C ↔ C_2R_1	K_A (M^{-1})	10,078	213
	ΔH (cal/mol)	816	3

forces were obtained as a function of the reaction coordinate shown in Figure S1. By integrating such forces, the PMF profiles were calculated (see Fig. 5). Those profiles exhibit a very high energy barrier for the entry of the drug by the primary side of the CD and a relatively broad and shallower well on the secondary side. This behaviour takes place for the three CDs with both relative orientations of the guest–host molecules. This means that the binding of remdesivir by the primary side of the CDs is unlikely. For the "up" orientation, a double minimum separated by an energy barrier is present for the three CDs, regardless the protonation state of the drug. The minimum at low ξ values corresponds to configurations where the remdesivir molecule is completely threading the CD (Figs. 6 and 7). The energy of this minimum is similar to that of the more external one, located at ξ ~ 0.8 nm for **7SBE** and **6SBE** with protonated remdesivir and for **6SBE** for neutral remdesivir. In the conformation corresponding to the external minima, the remdesivir molecule seems to interact directly with the SBE substituted groups. For both protonation states of the ligand the cyclodextrin with lower number of substitutions, **5SBE**, exhibits the less pronounced energy wells. The fact that the energy of the minimum corresponding to low ξ values is not very deep, together with the energy barrier separating both wells, is expected to make difficult to reach the actual inclusion complex. In the case of the "down" orientation the deepest minimum was observed only for **7SBE** interacting with neutral remdesivir. For the other two cyclodextrins, **5SBE** and **6SBE**, as well as for the three CDs interacting with protonated remdesivir, the PMF profile exhibits several fluctuations with a negative average slope when ξ decreases beyond the external minimum. There are several clear differences between the profiles corresponding to neutral and protonated remdesivir. The energy wells for the latter are clearly deeper than for the former. However, the structures corresponding to the minima do not seem to depend too much on the charge of remdesivir (Figs. 6 and 7). It is also worth to comment that the flat region in the PMF profile for neutral remdesivir is reached at much shorter distances than for the protonated structure, which still keeps a significant slope at ξ values larger than 2 nm. This is likely due to the electrostatic attraction between the CD and the charged drug in the second case.

As explained in the methods section, the PMF profile was employed to determine the association constants for the different CD structures. The association constant was calculated separately for the up and down orientations. Using the law for mass action, it can be easily demonstrated that the overall association constant can be obtained as the sum of the association constants obtained for the relative orientations (Table 3 and Fig. 8). The K_A values obtained for protonated remdesivir significantly depend on the number of substitutions. The value obtained for **5SBE** is of the same order of magnitude than that obtained by ITC at pH 3, while the K_A for the **6SBE** and **7SBE** is one order of magnitude larger. In contrast, the K_A values obtained for neutral remdesivir are very low, suggesting that the interaction is much weaker in this case. Although the ITC experiments at pH 6 are not conclusive, the low heat power signal is in agreement with this computational result. Interestingly, the fact that the CD structure with less number of

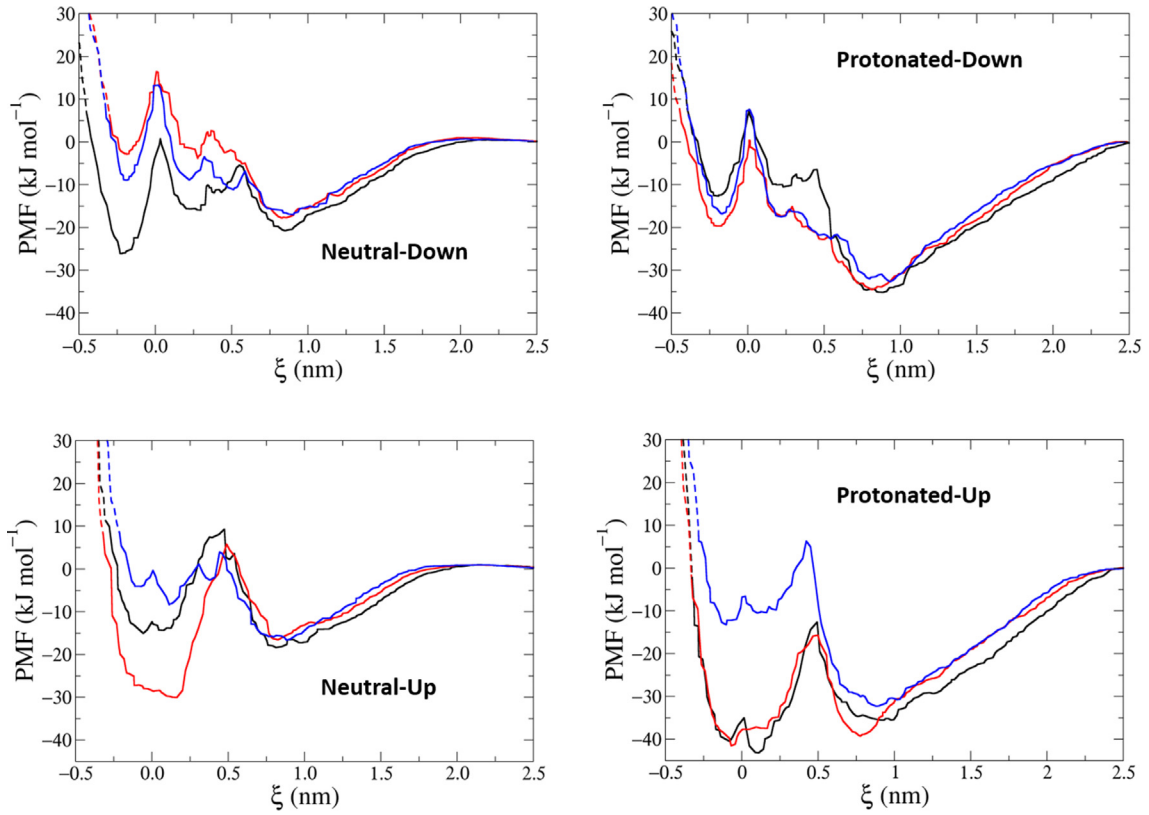

Fig. 5. Potential of mean force (PMF) profiles as a function of the reaction coordinate for the three cyclodextrin structures shown in Fig. 1 and neutral or protonated remdesivir considering both relative orientations. The profiles for **7SBE**, **6SBE** and **5SBE** are in black, red and blue solid lines, respectively. The dashed lines at low ξ values were included to highlight the large negative slope of the PMF in that region, due to the presence of a large energy barrier. (For interpretation of the references to color in this figure legend, the reader is referred to the web version of this article.)

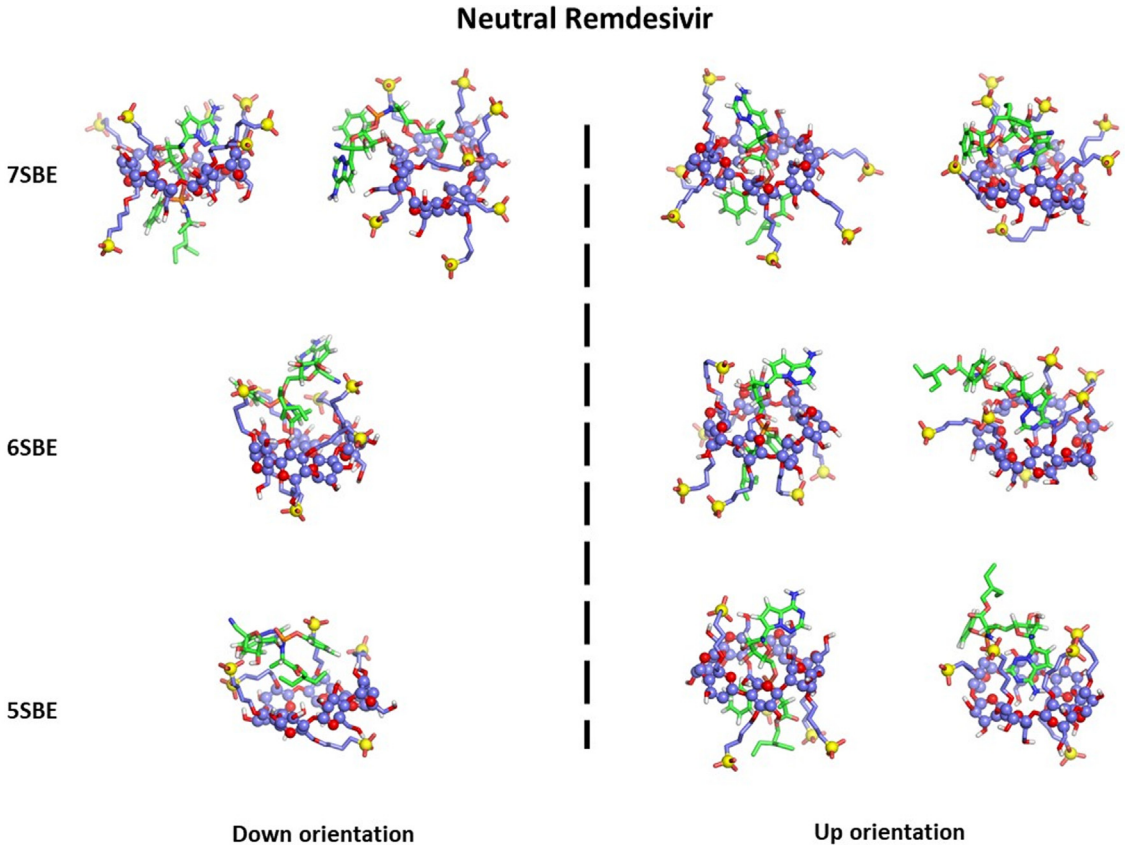

Fig. 6. Representative structures corresponding to the minimum of the PMF wells for the studied cyclodextrins and neutral remdesivir.

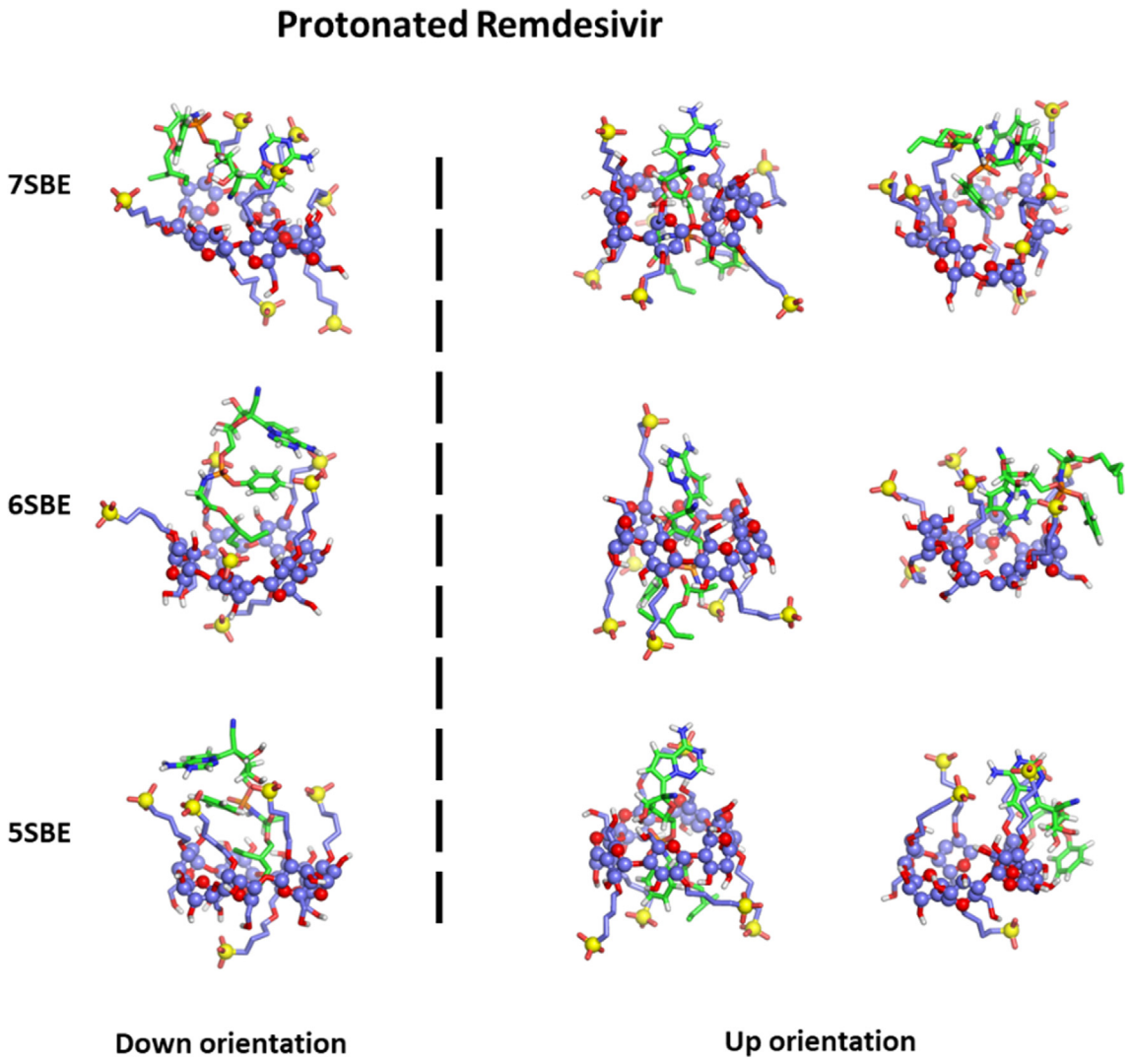

Fig. 7. Representative structures corresponding to the minimum of the PMF wells for the studied cyclodextrins and protonated remdesivir.

Table 3
Association constants obtained from the PMF profiles between the three CD structures shown in Fig. 1 and neutral or protonated remdesivir using Eq. (2).

Cyclodextrin	Neutral remdesivir			Protonated remdesivir		
	UP	DOWN	Overall	UP	DOWN	Overall
7SBE	76 ± 13	441 ± 164	517 ± 165	$(1.57 \pm 0.37)\cdot10^5$	$(1.88 \pm 0.58)\cdot10^4$	$(1.76 \pm 0.38)\cdot10^5$
6SBE	159 ± 81	61.2 ± 6.7	220 ± 81	$(3.1 \pm 1.7)\cdot10^5$	$(5.30 \pm 0.84)\cdot10^4$	$(3.6 \pm 1.7)\cdot10^5$
5SBE	29.4 ± 4.3	51.4 ± 6.1	80.8 ± 7.5	$(1.38 \pm 0.57)\cdot10^4$	$(3.33 \pm 1.8)\cdot10^4$	$(4.7 \pm 1.9)\cdot10^4$

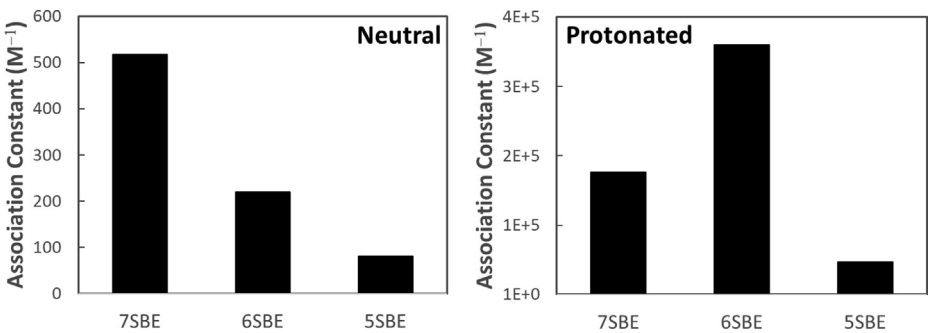

Fig. 8. Overall association constants obtained from the PMF profiles between the three CD structures shown in Fig. 1 and neutral or protonated remdesivir.

substitutions, **5SBE**, exhibits the lowest association constant agrees with the interpretation proposed for the r_C value obtained from the analysis of the ITC measurements, i.e. a significant dependence of the association constant with the SBE substitution pattern in the CD. Due to the high computational cost of these calculations, only three CD structures were tested, but the number of different molecules comprising CAPTISOL is huge, considering the possible combination of different substitution numbers and locations. Thus, the presence of other structures with lower and higher affinity constants is expected. This result is interesting not only for the interaction between CAPTISOL and remdesivir but also for other ligands.

The average forces calculated from 1-ns-long trajectory segments were used to get the corresponding PMF profiles (see Fig. S2) and the standard deviation of the association constants resulting from the application of Eq. (2) was taken as the uncertainty. Although the resulting values are large, the differences between the association constants obtained for the different cyclodextrins are significant. This supports the finding that the binding of remdesivir to **5SBE**, the CD with lowest number of substitutions, is weaker than for the other two CDs, **6SBE** and **7SBE**.

4. Conclusions

A structural and thermodynamic analysis for the interaction between CAPTISOL and neutral or protonated remdesivir has been performed using multiple ITC measurements and computational MD simulations. The global analysis of the calorimetric measurements suggests that a relatively strong complex with an association constant of ~ 10^4 is formed at pH 3. The need to introduce an extra parameter in the fitting model, accounting for the proportion of active CD, indicates that a large amount of structures do not effectively encapsulate the drug. The ITC measurements at neutral pH did not produce a strong signal. This could be due to a weak interaction under these conditions, but the analysis of the corresponding isotherms was not conclusive. At both pH values, the signal corresponding to the dilution of CAPTISOL was relatively large, comparable to the signal arising from the interaction with the drug molecule. The source of this signal deserves a further study but its large value indicates that it has to be considered in the analysis between CAPTISOL and remdesivir or other drugs. Since the analysis of ITC measurements provides global thermodynamics parameters for the whole distribution of CD structures consisting CAPTISOL, it does not provide information on which number and location of SBE substitutions favor the encapsulation of the drug. This has been further investigated by MD simulations using three different structures with 7, 6 and 5 SBE substitutions respectively. These simulations provided complete energy profiles for the encapsulation mechanism, indicating that the remdesivir molecule can spontaneously bind with the CD by the secondary side and, preferentially, with the "up" orientation. The entry of the drug by the primary side of the CD seems to be blocked by a high energy barrier for all the structures. Additionally, the simulations clearly indicate that the binding with the drug is significantly stronger when it is protonated (corresponding to low pH values) than when it is not charged (corresponding to neutral pH values). The values obtained for the association constants from the PMF profiles indicate that the binding is weaker for the structure with the lowest number of SBE substitutions, also in agreement with the ITC conclusion that the affinity is significantly dependent on the number and location of structures consisting CAPTISOL. Further studies using more CD structures with lower and higher number of substitutions, as well as using complementary experimental and computational methods would be useful to confirm our conclusions. Complementary studies considering several cyclodextrin and drug molecules in the same simulation box, in order to consider the impact of self-aggregation, would also be useful. Some recent computational investigations in this direction have recently been published [42]. Overall, our results suggest that pharmaceutical formulations based on excipients could be optimized by enriching the most active fractions. This would minimize eventual toxicity problems, and would possibly allow reducing the pharmaceutical doses for therapeutic treatments, in particular COVID-19.

CRediT authorship contribution statement

Ángel Piñeiro: Conceptualization, Methodology, Investigation, Writing – review & editing. **James Pipkin:** Conceptualization, Writing – review & editing. **Vince Antle:** Conceptualization, Writing – review & editing. **Rebeca Garcia-Fandino:** Conceptualization, Supervision, Writing – review & editing.

Declaration of Competing Interest

The authors declare that they have no known competing financial interests or personal relationships that could have appeared to influence the work reported in this paper.

Acknowledgements

R.G.-F thanks to the Spanish Agencia Estatal de Investigación (AEI) and the ERDF (RTI2018-098795-A-I00) and for a "Ramón y Cajal" contract (RYC-2016-20335), to Xunta de Galicia (ED431F 2020/05) and Centro singular de investigación de Galicia accreditation 2019-2022, ED431G 2019/03) and the European Union (European Regional Development Fund - ERDF). Á. P. thanks to the Ministerio de Ciencia e Innovación (PID2019-111327GB-I00). We thank the "Centro de Supercómputo de Galicia" (CESGA) for computing time as well as for their exceptional technical support.

Appendix A. Supplementary material

Supplementary data to this article can be found online at https://doi.org/10.1016/j.molliq.2021.117157.

References

[1] T.K. Warren, R. Jordan, M.K. Lo, A.S. Ray, R.L. Mackman, V. Soloveva, D. Siegel, M. Perron, R. Bannister, H.C. Hui, N. Larson, R. Strickley, J. Wells, K.S. Stuthman, S.A. Van Tongeren, N.L. Garza, G. Donnelly, A.C. Shurtleff, C.J. Retterer, D. Gharaibeh, R. Zamani, T. Kenny, B.P. Eaton, E. Grimes, L.S. Welch, L. Gomba, C.L. Wilhelmsen, D.K. Nichols, J.E. Nuss, E.R. Nagle, J.R. Kugelman, G. Palacios, E. Doerffler, S. Neville, E. Carra, M.O. Clarke, L. Zhang, W. Lew, B. Ross, Q. Wang, K. Chun, L. Wolfe, D. Babusis, Y. Park, K.M. Stray, I. Trancheva, J.Y. Feng, O. Barauskas, Y. Xu, P. Wong, M.R. Braun, M. Flint, L.K. McMullan, S.-S. Chen, R. Fearns, S. Swaminathan, D.L. Mayers, C.F. Spiropoulou, W.A. Lee, S.T. Nichol, T. Cihlar, S. Bavari, Therapeutic efficacy of the small molecule GS-5734 against Ebola virus in rhesus monkeys, Nature 531 (7594) (2016) 381–385, https://doi.org/10.1038/nature17180.

[2] T.P. Sheahan, A.C. Sims, R.L. Graham, V.D. Menachery, L.E. Gralinski, J.B. Case, S. R. Leist, K. Pyrc, J.Y. Feng, I. Trantcheva, R. Bannister, Y. Park, D. Babusis, M.O. Clarke, R.L. Mackman, J.E. Spahn, C.A. Palmiotti, D. Siegel, A.S. Ray, T. Cihlar, R. Jordan, M.R. Denison, R.S. Baric, Broad-spectrum antiviral GS-5734 inhibits both epidemic and zoonotic coronaviruses, Sci. Transl. Med. 9 (396) (2017) eaal3653, https://doi.org/10.1126/scitranslmed.aal3653.

[3] E. de Wit, F. Feldmann, J. Cronin, R. Jordan, A. Okumura, T. Thomas, D. Scott, T. Cihlar, H. Feldmann, Prophylactic and therapeutic remdesivir (GS-5734) treatment in the rhesus macaque model of MERS-CoV infection, Proc. Natl. Acad. Sci. U. S. A. 117 (12) (2020) 6771–6776, https://doi.org/10.1073/pnas.1922083117.

[4] W. Yin, C. Mao, X. Luan, D.D. Shen, Q. Shen, H. Su, X. Wang, F. Zhou, W. Zhao, M. Gao, S. Chang, Y.C. Xie, G. Tian, H.W. Jiang, S.C. Tao, J. Shen, Y. Jiang, H. Jiang, Y. Xu, S. Zhang, Y. Zhang, H.E. Xu, Structural basis for the inhibition of the RNA-Dependent RNA polymerase from SARS-CoV-2 by Remdesivir, BioRxiv. (2020), https://doi.org/10.1101/2020.04.08.032763.

[5] G. Kokic, H.S. Hillen, D. Tegunov, C. Dienemann, F. Seitz, J. Schmitzova, L. Farnung, A. Siewert, C. Höbartner, P. Cramer, Mechanism of SARS-CoV-2 polymerase stalling by remdesivir, Nat. Commun. 12 (1) (2021), https://doi.org/10.1038/s41467-020-20542-0.

[6] C.J. Gordon, E.P. Tchesnokov, E. Woolner, J.K. Perry, J.Y. Feng, D.P. Porter, M. Götte, Remdesivir is a direct-acting antiviral that inhibits RNA-dependent RNA polymerase from severe acute respiratory syndrome coronavirus 2 with high potency, J. Biol. Chem. 295 (20) (2020) 6785–6797, https://doi.org/10.1074/jbc.RA120.013679.
[7] E. Mahase, Covid-19: Remdesivir probably reduces recovery time, but evidence is uncertain, panel finds, BMJ 370 (2020), https://doi.org/10.1136/bmj.m3049 m3049.
[8] J.H. Beigel, K.M. Tomashek, L.E. Dodd, A.K. Mehta, B.S. Zingman, A.C. Kalil, E. Hohmann, H.Y. Chu, A. Luetkemeyer, S. Kline, D. Lopez de Castilla, R.W. Finberg, K. Dierberg, V. Tapson, L. Hsieh, T.F. Patterson, R. Paredes, D.A. Sweeney, W.R. Short, G. Touloumi, D.C. Lye, N. Ohmagari, M.-D. Oh, G.M. Ruiz-Palacios, T. Benfield, G. Fätkenheuer, M.G. Kortepeter, R.L. Atmar, C.B. Creech, J. Lundgren, A.G. Babiker, S. Pett, J.D. Neaton, T.H. Burgess, T. Bonnett, M. Green, M. Makowski, A. Osinusi, S. Nayak, H.C. Lane, Remdesivir for the Treatment of Covid-19 — Final Report, N. Engl. J. Med. 383 (19) (2020) 1813–1826, https://doi.org/10.1056/NEJMoa2007764.
[9] R. Zampino, F. Mele, L.L. Florio, L. Bertolino, R. Andini, M. Galdo, R. De Rosa, A. Corcione, E. Durante-Mangoni, Liver injury in remdesivir-treated COVID-19 patients, Hepatol. Int. 14 (5) (2020) 881–883, https://doi.org/10.1007/s12072-020-10077-3.
[10] P.F. Garrido, M. Calvelo, A. Blanco-González, U. Veleiro, F. Suárez, D. Conde, A. Cabezón, Á. Piñeiro, R. Garcia-Fandino, The Lord of the NanoRings: Cyclodextrins and the battle against SARS-CoV-2, Int. J. Pharm. 588 (2020) 119689, https://doi.org/10.1016/j.ijpharm.2020.119689.
[11] M.V. Ol'khovich, A.V. Sharapova, G.L. Perlovich, S.Y. Skachilova, N.K. Zheltukhin, Inclusion complex of antiasthmatic compound with 2-hydroxypropyl-β-cyclodextrin: Preparation and physicochemical properties, J. Mol. Liq. 237 (2017) 185–192, https://doi.org/10.1016/j.molliq.2017.04.098.
[12] G. Singh, P.K. Singh, Complexation of a cationic pyrene derivative with sulfobutylether substituted β-cyclodextrin: Towards a stimulus-responsive supramolecular material, J. Mol. Liq. 305 (2020) 112840, https://doi.org/10.1016/j.molliq.2020.112840.
[13] A. Joardar, G. Meher, B.P. Bag, H. Chakraborty, Host-guest complexation of eugenol in cyclodextrins for enhancing bioavailability, J. Mol. Liq. 319 (2020) 114336, https://doi.org/10.1016/j.molliq.2020.114336.
[14] N. Nasongkla, A.F. Wiedmann, A. Bruening, M. Beman, D. Ray, W.G. Bornmann, D.A. Boothman, J. Gao, Enhancement of Solubility and Bioavailability of β-Lapachone Using Cyclodextrin Inclusion Complexes, Pharm. Res. 20 (2003) 1626–1633, https://doi.org/10.1023/A:1026143519395.
[15] K. Uekama, Y. Hieda, F. Hirayama, H. Arima, M. Sudoh, A. Yagi, H. Terashima, Stabilizing and Solubilizing Effects of Sulfobutyl Ether β-Cyclodextrin on Prostaglandin E1 Analogue, Pharm. Res. 18 (2001) 1578–1585, https://doi.org/10.1023/A:1013034615464.
[16] T. Musumeci, A. Bonaccorso, F. De Gaetano, K.L. Larsen, R. Pignatello, A. Mazzaglia, G. Puglisi, C.A. Ventura, A physico-chemical study on amphiphilic cyclodextrin/liposomes nanoassemblies with drug carrier potential, J. Liposome Res. 30 (4) (2020) 407–416, https://doi.org/10.1080/08982104.2019.1682603.
[17] A. Mazzaglia, R. Donohue, B.J. Ravoo, R. Darcy, Novel Amphiphilic Cyclodextrins: Graft-Synthesis of Heptakis(6-alkylthio-6-deoxy)-β-cyclodextrin 2-Oligo(ethylene glycol) Conjugates and Their ω-Halo Derivatives, Eur. J. Org. Chem. 2001 (2001) 1715–1721, https://doi.org/10.1002/1099-0690(200105)2001:9<1715::AID-EJOC1715>3.0.CO;2-A.
[18] V. Zia, R.A. Rajewski, V.J. Stella, Effect of Cyclodextrin Charge on Complexation of Neutral and Charged Substrates: Comparison of (SBE)7M-β-CD to HP-β-CD, Pharm. Res. 18 (2001) 667–673, https://doi.org/10.1023/A:1011041628797.
[19] V. Zia, R.A. Rajewski, V.J. Stella, Thermodynamics of Binding of Neutral Molecules to Sulfobutyl Ether β-Cyclodextrins (SBE-β-CDs): The Effect of Total Degree of Substitution, Pharm. Res. 17 (2000) 936–941, https://doi.org/10.1023/A:1007571019908.
[20] V.C. Yan, F.L. Muller, Captisol and GS-704277, but Not GS-441524, Are Credible Mediators of Remdesivir's Nephrotoxicity, Antimicrob. Agents Chemother. 64 (12) (2020), https://doi.org/10.1128/AAC.01920-20.
[21] M.P. Lê, C. Le Beller, Q. Le Hingrat, P. Jaquet, P.-H. Wicky, V. Bunel, L. Massias, B. Visseaux, J. Messika, D. Descamps, H. Mal, J.-F. Timsit, G. Peytavin, Reply to Yan and Muller, "Captisol and GS-704277, but Not GS-441524, Are Credible Mediators of Remdesivir's Nephrotoxicity", Antimicrob. Agents Chemother. 64 (2020), https://doi.org/10.1128/AAC.01937-20.
[22] N. Larson, Compositions comprising an rna polymerase inhibitor and cyclodextrin for treating viral infections, US 2019/0083525 A1, 2019.
[23] D.-Y. Ma, Y.-M. Zhang, J.-N. Xu, The synthesis and process optimization of sulfobutyl ether β-cyclodextrin derivatives, Tetrahedron. 72 (22) (2016) 3105–3112, https://doi.org/10.1016/j.tet.2016.04.039.
[24] Q.I. Qu, E. Tucker, S.D. Christian, Sulfoalkyl Ether β-Cyclodextrin Derivatives: Synthesis and Characterizations, J. Incl. Phenom. Macrocycl. Chem. 43 (2002) 213–222, https://doi.org/10.1023/A:1021255314835.
[25] P.F. Garrido, M. Calvelo, R. Garcia-Fandiño, Á. Piñeiro, Rings, hexagons, petals, and dipolar moment sink-sources: The fanciful behavior of water around cyclodextrin complexes, Biomolecules 10 (2020) 431, https://doi.org/10.3390/biom10030431.
[26] E. Mixcoha, J. Campos-Terán, Á. Piñeiro, Surface adsorption and bulk aggregation of cyclodextrins by computational molecular dynamics simulations as a function of temperature: α-CD vs β-CD, J. Phys. Chem. B. 118 (25) (2014) 6999–7011, https://doi.org/10.1021/jp412533b.
[27] N. Schmid, A.P. Eichenberger, A. Choutko, S. Riniker, M. Winger, A.E. Mark, W.F. van Gunsteren, Definition and testing of the GROMOS force-field versions 54A7 and 54B7, Eur. Biophys. J. 40 (7) (2011) 843–856, https://doi.org/10.1007/s00249-011-0700-9.
[28] H.J.C. Berendsen, J.P. Postma, W.F. van Gunsteren, J. Hermans, Interaction Models for Water in Relation to Protein HydrationIn, in: B. Pullman (Ed.), Intermol, Forces, Dordrecht, 1981, pp. 331–342.
[29] H.J.C. Berendsen, D. van der Spoel, R. van Drunen, GROMACS: A message-passing parallel molecular dynamics implementation, Comput. Phys. Commun. 91 (1-3) (1995) 43–56, https://doi.org/10.1016/0010-4655(95)00042-E.
[30] M.J. Abraham, T. Murtola, R. Schulz, S. Páll, J.C. Smith, B. Hess, E. Lindah, Gromacs: High performance molecular simulations through multi-level parallelism from laptops to supercomputers, SoftwareX 1–2 (2015) 19–25, https://doi.org/10.1016/j.softx.2015.06.001.
[31] G. Bussi, D. Donadio, M. Parrinello, Canonical sampling through velocity rescaling, J. Chem. Phys. 126 (1) (2007) 014101, https://doi.org/10.1063/1.2408420.
[32] M. Parrinello, A. Rahman, Polymorphic transitions in single crystals: A new molecular dynamics method, J. Appl. Phys. 52 (12) (1981) 7182–7190, https://doi.org/10.1063/1.328693.
[33] U. Essmann, L. Perera, M.L. Berkowitz, T. Darden, H. Lee, L.G. Pedersen, A smooth particle mesh Ewald method, J. Chem. Phys. 103 (19) (1995) 8577–8593, https://doi.org/10.1063/1.470117.
[34] T. Darden, D. York, L. Pedersen, Particle mesh Ewald: An N·log(N) method for Ewald sums in large systems, J. Chem. Phys. 98 (12) (1993) 10089–10092, https://doi.org/10.1063/1.464397.
[35] R.W. Hockney, J.W. Eastwood, Computer Simulation Using Particles, McGraw-Hill International Book Company, 1981.
[36] S. Miyamoto, P.A. Kollman, SETTLE: An Analytical Version of the SHAKE and RATTLE Algorithm for Rigid Water Models, J. Comput. Chem. 13 (8) (1992) 952–962, https://doi.org/10.1002/(ISSN)1096-987X10.1002/jcc.v13:810.1002/jcc.540130805.
[37] B. Hess, H. Bekker, H.J.C. Berendsen, J.G.E.M. Fraaije, LINCS: A linear constraint solver for molecular simulations, J. Comput. Chem. 18 (1997) 1463–1472, https://doi.org/10.1002/(SICI)1096-987X(199709)18:12<1463::AID-JCC4>3.0.CO;2-H.
[38] J. Comer, J.C. Gumbart, J. Hénin, T. Lelièvre, A. Pohorille, C. Chipot, The adaptive biasing force method: Everything you always wanted to know but were afraid to ask, J. Phys. Chem. B. 119 (3) (2015) 1129–1151, https://doi.org/10.1021/jp506633n.
[39] Y. Yu, C. Chipot, W. Cai, X. Shao, Molecular dynamics study of the inclusion of cholesterol into cyclodextrins, J. Phys. Chem. B. 110 (12) (2006) 6372–6378, https://doi.org/10.1021/jp056751a.
[40] D. Shoup, A. Szabo, Role of diffusion in ligand binding to macromolecules and cell-bound receptors, Biophys. J. 40 (1) (1982) 33–39, https://doi.org/10.1016/S0006-3495(82)84455-X.
[41] Á. Piñeiro, E. Muñoz, J. Sabín, M. Costas, M. Bastos, A. Velázquez-Campoy, P.F. Garrido, P. Dumas, E. Ennifar, L. García-Río, J. Rial, D. Pérez, P. Fraga, A. Rodríguez, C. Cotelo, AFFINImeter: A software to analyze molecular recognition processes from experimental data, Anal. Biochem. 577 (2019) 117–134, https://doi.org/10.1016/j.ab.2019.02.031.
[42] G. Raffaini, F. Ganazzoli, Understanding Surface Interaction and Inclusion Complexes between Piroxicam and Native or Crosslinked β-Cyclodextrins: The Role of Drug Concentration, Mol. 25 (12) (2020) 2848, https://doi.org/10.3390/molecules25122848.